Journal of Nuclear Medicine, published on November 16, 2017 as doi:10.2967/jnumed.117.202010

First-in-human HER2-targeted imaging using ^{89}Zr-pertuzumab PET/CT: Dosimetry and clinical application in patients with breast cancer

Gary A. Ulaner[1,2], Serge K. Lyashchenko[1,2], Christopher Riedl[1,2], Shutian Ruan[3], Pat B. Zanzonico[3], Diana Lake[4,5], Komal Jhaveri[4,5], Brian Zeglis[6], Jason S. Lewis[1,2,7], Joseph A. O'Donoghue[3]

Departments of [1]Radiology, [3]Medical Physics, and [4]Medicine, Memorial Sloan Kettering Cancer Center, New York, NY, USA

Departments of [2]Radiology and [5]Medicine, Weill Cornell Medical College, New York, NY, USA

[6]Department of Chemistry, Hunter College, New York, NY, USA

[7]Program in Molecular Pharmacology, Memorial Sloan Kettering Cancer Center, New York, NY, USA.

Corresponding Author: Gary A Ulaner, MD, PhD, Memorial Sloan Kettering Cancer Center, 1275 York Ave, Box 77, New York, NY 10065. Phone: (212) 639-3776. Fax: (212) 717-3263. E-mail: ulanerg@mskcc.org

Manuscript Type: Original Research

Word Count: 4,972 (maximum 5,000)

Running Title: First-in-human Zr-pertuzumab PET/CT

ABSTRACT

In this first-in-human study, we evaluate the safety and dosimetry of ^{89}Zr-pertuzumab PET/CT (Positron Emission Tomography / Emission Tomography) for HER2 (Human epidermal growth factor receptor 2)-targeted imaging in patients with HER2-postive breast cancer.

Materials and Methods: Patients with HER2-positive breast cancer and evidence of distant metastases were enrolled in an Institutional Review Board-approved prospective clinical trial. Pertuzumab was conjugated with deferoxamine and radiolabeled with ^{89}Zr. Patients underwent ^{89}Zr-pertuzumab PET/CT with 74 MBq of ^{89}Zr-pertuzumab in a total antibody mass of 20-50 mg of pertuzumab. PET/CT, whole-body probe counts, and blood draws were performed over 8 days to assess pharmacokinetics, biodistribution, and dosimetry. PET/CT images were evaluated for ability to visualize HER2-positive metastases.

Results: Six patients with HER2-positive metastatic breast cancer were enrolled and administered ^{89}Zr-pertuzumab. No toxicities occurred. Dosimetry estimates from Organ Level Internal Dose Assessment (OLINDA) demonstrated the organs receiving the highest doses (mGy/MBq) were liver (1.75 ± 0.21), kidneys (1.27 ± 0.28), and heart wall (1.22 ± 0.16) with an average effective dose of 0.54 ± 0.07 mSv/MBq. PET/CT demonstrated optimal imaging 5-8 days post-administration. ^{89}Zr-pertuzumab was able to image multiple sites of malignancy, and suggest they are HER2-positive. In two patients with both known HER2-positive and HER2-negative primary breast cancers and brain metastases, ^{89}Zr-pertuzumab PET/CT suggested the brain metastases were HER2-positive. In one of two patients, subsequent resection of a brain metastasis proved HER2-positive disease, confirming ^{89}Zr-pertuzumab-avidity was true positive for HER2-positive malignancy.

Conclusion: This first-in-human study demonstrated safety, dosimetry, biodistribution, and successful HER2-targeted imaging with ^{89}Zr-pertuzumab PET/CT. Potential clinical applications

include assessment of HER2 status of lesions which may not be accessible to biopsy and assessment of HER2 heterogeneity.

INTRODUCTION

Human epidermal growth factor receptor 2 (HER2) is a critical biomarker in breast cancer, and its expression directly influences treatment. Approximately 20% of invasive ductal breast malignacies are classified as HER2-positive as a result of *ERBB2* gene amplification and/or the subsequent overexpression of the HER2 protein on the surface of tumor cells (*1*). Patients with HER2-positive breast cancer receive specific therapies targeted to HER2 that reduce the risk of death, while patients with HER2-negative breast cancer do not receive them (*2,3*). This has resulted in considerable interest in HER2-targeted imaging (*4*). Recent work has demonstrated the ability to detect HER2-positive metastases in patients with HER2-negative primary breast tumors both by HER2-targeted imaging confirmed with immunohistochemistry (*5,6*) and molecular analyses (*7*). Thus, the ability to perform non-invasive, whole body, targeted HER2 imaging may be valuable in the detection of otherwise unsuspected HER2-positive malignancy and may help direct patients to appropriate HER2-targeted therapy.

While there have been successes in HER2-targeted imaging with ^{89}Zr-trastuzumab, there have also been examples of non-specific visualization of malignancy that is HER2-negative on pathology (*5,6*). More specific HER2-targeted agents may be needed for clinical translation of HER2-targeted imaging agents. Pertuzumab is a newer humanized monoclonal antibody that binds to the HER2 receptor at a site distinct from trastuzumab and appears to be more efficient than trastuzumab (*8*). *In vitro* and *in vivo* models have demonstrated successful ^{89}Zr-pertuzumab targeting to HER2-positive malignancy, and have notably demonstrated increased affinity for HER2 in the presence of trastuzumab (*9*), as may be the case in patients with HER2-positive malignancies receiving trastuzumab. Here we present our results from first-in-human HER2-

targeted imaging with ^{89}Zr-pertuzumab PET/CT, in order to document safety, dosimetry, and potential clinical utility of this HER2-targeted imaging agent.

MATERIALS AND METHODS

Patients

This study was performed under a single-center prospective Memorial Sloan Kettering Cancer Center Institutional Review Board-approved protocol (ClinicalTrials.gov identifier NCT03109977). All patients provided written informed consent. Patients with pathologically proven HER2-positive metastatic breast cancer were identified as potential candidates. HER2 positivity was defined according to American Society of Clinical Oncology guidelines (*10*), including 3+ HER2 immunohistochemistry (IHC) or 2+ HER2 IHC with ≥ 2.0 HER2 amplification on fluorescence in situ hybridization (FISH); 0 or 1+ IHC or 2+ IHC with < 2.0 HER2 amplification on FISH was considered HER2-negative. Inclusion criteria were: 1) biopsy-proven, HER2-positive malignancy, 2) foci of malignancy on imaging within 60 days of enrollment, 3) women age > 21, and 4) Eastern Cooperative Oncology Group performance score of 0-2. Exclusion criteria were: 1) life expectancy < 3months, 2) pregnancy or lactation, and 3) inability to undergo PET/CT scanning because of weight limits. Biopsies demonstrating HER2-positive malignancy were required for inclusion. The HER2-positive biopsy was allowed at any time of the patient's disease course, and was allowed from the primary breast malignancy or a site of metastatic disease. Patients were allowed to be on HER2 directed therapy. Sites of known malignancy were determined by medical imaging, including CT, MR, and 18F-Fluorodeoxyglucose (18F-FDG) PET/CT, within 60 days of protocol enrollment. The primary

malignancy and at least one site of distant metastasis were pathological proven as part of inclusion criteria.

^{89}Zr-pertuzumab

The ^{89}Zr-DFO-pertuzumab was manufactured at the MSK Radiochemistry and Molecular Imaging Probes Core Facility in compliance with the requirements specified in the Chemistry, Manufacturing, and Controls section of an United Stated Food and Drug Administration-acknowledged Investigational New Drug application (#134411). The preparation process involved conjugating clinical-grade pertuzumab (Perjeta, Genentech, South San Francisco, CA) with a bifunctional chelator, p-SCN-Bn-Deferoxamine (Macrocylics, Plano, TX), followed by radiolabeling with ^{89}Zr, a radiometal positron emitter with a 78.4-hour radioactive half-life. The conjugation and radiolabeling were performed using methodology previously described (*11*). Radiolabeling with ^{89}Zr was chosen based on this metallo-radionuclide's favorable properties such as radioactive half-life, which is long enough to allow for imaging of radiolabeled antibodies after localization at the target site has occurred, as well as mild radiolabeling conditions (at ambient temperature in 1M ammonium acetate buffer, pH7), which help to preserve pertuzumab protein integrity and immunoreactivity during the radiolabeling process (*12,13*). The ^{89}Zr-DFO pertuzumab final drug product batches underwent quality control testing prior to batch release for patient administration, in order to ensure conformance to the following acceptance specifications: radiochemical purity as determined by radio thin layer chromatography and size exclusion high-performance liquid chromatography; radio-immunoreactivity, as determined by using a live antigen expressing cell binding assay; endotoxin content, as measured by the portable test system supplied by Charles River Laboratories

(Wilmington, Massachusetts, USA); sterilizing filter integrity, as measured by the bubble point method; pH as measured by pH strips; appearance as a clear and particle free-solution, as determined by visual inspection check; and radionuclidic identity verification, as measured by radioactive gamma spectroscopy. Sterility testing, using the direct media inoculation method, was performed post-release.

^{89}Zr-pertuzumab Administration

An intravenous line was established and flushed with 5% human serum albumin solution. An amount of 18 or 48 mg of non-radiolabeled pertuzumab was then intravenously administered over 5 minutes. Cold pertuzumab was administered to help reduce non-specific uptake of the subsequent radiolabeled pertuzumab. Then 74 MBq +/- 10% of ^{89}Zr-pertuzumab was intravenously administered in a mass of approximately 2 mg, to bring the total pertuzumab antibody mass to 20 or 50 mg for each patient. The first two patients were administered 50 mg, then antibody mass was reduced to 20 mg for the next two patients. Visual analysis suggested 50 mg total antibody mass produced lower background uptake, thus the total antibody mass was increased back to 50 mg for the final two patients. Patients were monitored for side effects on the day of and the day after ^{89}Zr-pertuzumab administration.

^{89}Zr-pertuzumab PET/CT and Image Analysis

Up to four whole body PET/CT scans were obtained for each patient on days 1, 2-4, 5-6, and 7-8 following administration (day 0) of ^{89}Zr-pertuzumab. Ranges for days of imaging were preselected before opening the protocol to allow both comprehensive multiday imaging and flexibility of scheduling, particularly over the weekend.

Patients were imaged from skull apex to mid-thigh on a dedicated research PET/CT scanner (GE Discovery 710) in 3D mode with emission time per bed position extending from 4 min (day 1) to 8 min (day 7-8). Low dose CT scans were acquired with an x-ray tube current of 80 mA. PET/CT images were reconstructed with attenuation, scatter, and other standard corrections applied and using iterative reconstruction. ^{89}Zr-pertuzumab PET/CT scans were interpreted by a nuclear radiologist with experience in HER2-targeted imaging (GAU) and knowledge of the patient's medical history and prior imaging. Non-physiologic radiotracer uptake was considered suspicious for HER2-positive malignancy. Volumes of interest were drawn on PET/CT images over normal liver, kidney, spleen, and lung using a dedicated workstation (Hermes Medical Solution, Stockholm, Sweden). Normal tissue uptake was quantified by mean standardized uptake value adjusted to lean body mass (SUV_{LBM}).

Whole-body and Serum Clearance Measurements

Whole-body clearance was determined by serial measurements of count-rate using a 12.7 cm-thick sodium iodide NaI (Tl) scintillation detector at a fixed 3 m from the patient. Background-corrected geometric mean counts were obtained after infusion before and after first voiding and subsequently at the times of the PET scans (n=6). Count rates were normalized to the immediate post-infusion value (taken as 100%) to yield relative retained activities (in %). Multiple blood samples were obtained at approximately 15 min, 30 min, and 1-2 h after injection, and subsequently at the times of each PET scan (n=7). Aliquots of serum were counted using a gamma well-type detector (Wallac Wizard 1480 gamma counter, Perkin Elmer) and measured activity concentrations converted to percent injected activity/liter (% IA/L).

A mono-exponential function was fitted to the whole-body probe data and a bi-exponential function fitted to the serum activity concentration data using SAAM software (*14*). Areas under the curve (AUC) and corresponding residence times were derived by analytic integration.

Normal Tissue Dosimetry

Normal tissue dose estimates were derived as described previously (*15,16*). Briefly, image-derived SUV_{LBM} were converted to activity concentration per unit mass (kBq/g) and AUC estimated by trapezoidal integration. Whole-organ AUCs were estimated by multiplying the activity concentration AUC by projected organ mass. Residence times were derived by dividing whole organ AUC by the administered activity. Corresponding values for heart contents and red marrow were estimated from the serum AUC (*17*). The residence time for the remainder of body was derived by subtracting all individually estimated residence times from the WB residence time. Thereafter, absorbed radiation doses to individual organs were calculated using the OLINDA/EXM software application (*18*).

Comparison of 89Zr-pertuzumab Dosimetry with 89Zr-trastuzumab Dosimetry

Tissue and total body dosimetry was compared for the newly calculated values for 89Zr-pertuzumab and published values for 89Zr-trastuzumab.

Statistics

Kinetic parameters and absorbed dose estimates were calculated for each patient on an individual basis. Subsequently, these were summarized using descriptive statistics.

RESULTS

Patient Characteristics

Between April and June 2017, six patients, all women with biopsy-proven HER2-positive malignancy from invasive ductal breast cancer (IDC), completed the study protocol. All patients underwent imaging on days 1, 2-4, 5-6, and/or 7-8, as prescribed prospectively in the protocol. Patient characteristics are summarized in Table 1.

Sites of Known Malignancy at Time of Protocol Enrollment

Sites of known malignancy were determined from medical imaging within 60 days of protocol enrollment. Known nodal disease was present in four patients, brain malignancy in two, hepatic malignancy in two, and malignancy involving the breast, bone, chest wall, and lung each in one patient. Sites of known malignancy are summarized in Table 1.

Adverse Events

All six patients underwent ^{89}Zr-pertuzumab administration. Patients were monitored for two hours after tracer injection, as well as evaluated the following day when they returned for PET/CT imaging, and no side effects were observed or reported. Vital signs were recorded before and after tracer administration and there were no changes with clinical significance. Safety data were reviewed and approved by the US Food and Drug Administration as part of an Investigational New Drug application.

Pharmacokinetics

Whole body and serum clearance conformed to mono- and bi-exponential kinetics, respectively. Summed biologic clearance curves are shown in Figure 1. Summary statistics for the clearance parameters are provided in Table 2.

Biodistribution and Normal Tissue Dose Estimates

^{89}Zr-pertuzumab uptake was observed in the blood pool, liver, kidney, and spleen. There was little measureable change in whole body activity following the first void (98% ± 1.8 of pre-void measurement). The urinary bladder was not visualized on any PET/CT scan. Bowel excretion was visualized in two patients on day 1 and 2 scans. Uptake in liver and kidneys in terms of SUV_{LBM} was relatively constant over the duration of imaging, whereas blood pool and spleen uptake decreased over time. These sites of tracer visualization were considered physiologic. Absorbed dose estimates for normal tissues are provided in Table 3. The organs receiving the highest doses (mGy/MBq) were liver (1.75 ± 0.21), kidneys (1.27 ± 0.28), and heart wall (1.22 ± 0.16), with an average effective dose of 0.54 ± 0.07 mSv/MBq.

Comparison of 89Zr-pertuzumab Dosimetry with 89Zr-trastuzumab Dosimetry

The mean effective dose of ^{89}Zr-pertuzumab was 0.54 mSv/MBq. Figure 2 shows the comparative absorbed dose estimates for both antibodies.

Imaging of Lesions with ^{89}Zr-pertuzumab PET/CT

Patient 1 had two known primary breast malignancies, a right breast estrogen receptor (ER), progesterone receptor (PR), and HER2-positive (HER2 IHC 3+) IDC diagnosed in 2014 and the other ER, PR, and HER2-negative (HER2 IHC 0) IDC diagnosed in 2015. She had

received HER2 directed therapy, including TDM-1 in 2015 and was currently on trastuzumab therapy at the time of the ^{89}Zr-pertuzumab PET/CT. She had a recent diagnosis of brain metastases. ^{89}Zr-pertuzumab PET/CT demonstrated progressive increase in ^{89}Zr-pertuzumab avidity over PET/CT scans obtained on days 1, 2, 6, and 8 following tracer administration (SUVmax of the most avid lesion was 13.6, 16.6, 26.0, and 30.1 on these four days; see Fig. 3A-D). Blood pool activity, including activity in the superior sagittal sinus, demonstrated continued decrease over the scans. This allowed most optimal visualization of the known brain metastases (Fig. 3E) on the day 8 scan (Fig. 3F).

Patient 2 had a left breast ER, PR, and HER2+ (HER2 IHC 2+, HER2 amplification 4.0 on FISH) IDC diagnosed in 2014. She had received HER2 directed therapy, including TDM-1 in 2015-2016 and was currently on trastuzumab and pertuzumab therapy at the time of the ^{89}Zr-pertuzumab PET/CT. She had known supraclavicular nodal metastases at the time of ^{89}Zr-pertuzumab PET/CT. There was relatively stable ^{89}Zr-pertuzumab avidity on days 1, 2, 5, and 7 following tracer administration (SUVmax of the most avid lesion was 6.0, 4.7, 4.6, and 5.1 on these four days).

Patient 3 had a left breast ER, PR, and HER3+ (HER2 IHC 3+) IDC diagnosed in 2014, which was metastatic to the lung at the time of diagnosis. She had received HER2 directed therapy, including trastuzumab and pertuzumab, which she was receiving at the time of the ^{89}Zr-pertuzumab PET/CT. At the time of ^{89}Zr-pertuzumab PET/CT, she had demonstrable 18F-FDG-avid disease in the left breast and left axillary nodes. There was mildly increasing ^{89}Zr-pertuzumab avidity on days 1, 2, 6, and 7 following tracer administration (SUVmax of the breast

lesion was 3.7, 4.7, 6.3, and 5.5). Decreasing background avidity made the avid lesions best visible on the day 6 and 7 scans (Fig. 4). ^{89}Zr-pertuzumab avidity was similar to 18F-FDG avidity (SUVmax 6.6), which was performed 3 weeks prior.

Patient 4 was diagnosed with ER-positive, HER2-negative (HER2 IHC 1+) in 2003. At the time of ^{89}Zr-pertuzumab PET/CT, she had demonstrable disease in the liver, bone, and chest wall on CT and MR. She had previously received HER2 directed therapy, including trastuzumab and pertuzumab, which she was receiving at the time of the ^{89}Zr-pertuzumab PET/CT. A recent biopsy of a right chest wall mass was HER2-positive (HER2 IHC 2+, HER2 amplification 2.4 on FISH). There was low-level avidity in the right chest wall lesion (SUVmax 2.8, 2.3, 2.4, and 2.4 on days 1, 4, 5, and 8 post-^{89}Zr-pertuzumab administration).

Patient 5 was diagnosed with two distinct right breast malignancies in 2014 and an ER-negative, HER2-positive (HER2 IHC 3+) malignancy, as well as an ER-positive, HER2-negative (HER2 IHC 0) malignancy. She had previously received HER2 directed therapy, including trastuzumab and pertuzumab, which she was receiving at the time of the ^{89}Zr-pertuzumab PET/CT. At the time of ^{89}Zr-pertuzumab PET/CT, she had demonstrable disease in the brain, lung, nodes, and liver. There was mild ^{89}Zr-pertuzumab avidity in the brain, lung, and nodal lesions, and was greatest in the brain (SUVmax of the most avid brain lesion was 2.9, 6.1, and 6.1 on days 1, 2, and 5 post-tracer administration). A brain metastasis was resected and was HER2-positive (IHC 2+, HER2 amplification 2.4 on FISH), confirming this was a site ^{89}Zr-pertuzumab-avidity which was true positive for HER2-positive malignancy. Liver lesions were not appreciably ^{89}Zr-pertuzumab-avid above liver background.

Patient 6 had a right breast ER-negative, HER2-positive (HER2 IHC 3+) IDC diagnosed in 2008. She had previously received HER2 directed therapy, including trastuzumab and pertuzumab, and was currently on TDM-1 therapy at the time of the ^{89}Zr-pertuzumab PET/CT. At the time of ^{89}Zr-pertuzumab PET/CT, she had only small volume disease in thoracic and abdominal nodes. Avidity in small nodes, greatest 1.5 x 1.2 cm in the right common iliac chain, was difficult to appreciate on ^{89}Zr-pertuzumab PET/CT.

DISCUSSION

This first-in-human trial demonstrates safety and dosimetry for intravenously administered ^{89}Zr-pertuzumab, which has been reviewed and accepted by the US Food and Drug Administration. We have also demonstrated successful HER2-targeted imaging in patients with HER2-positive metastatic breast cancer.

The mean effective dose of ^{89}Zr-pertuzumab was 0.54 mSv/MBq, which is comparable with other radiolabeled antibody PET tracers such as ^{89}Zr-J591 (0.38 mSv/MBq) (*15*). In particular, the biodistribution and normal tissue dosimetry for ^{89}Zr-pertuzumab is comparable with ^{89}Zr-trastuzumab (0.48 mSv/MBq) (*16*). However, ^{89}Zr-pertuzumab does appear to have slightly higher uptake in the central parenchymal organs (liver, kidney, spleen, and lung) than ^{89}Zr-trastuzumab; this translates into a higher (mGy/MBq) dose by an average factor of approximately 1.3 for these organs. Due to their relatively slow kinetics, antibody-based PET tracers require radionuclides with relatively long physical half-lives. This leads to higher

radiation doses than small molecule imaging agents that have fast kinetics and can use radionuclides with relatively short physical half-times — the classic example of which is ^{18}F-FDG. In this study, we used a lower activity of ^{89}Zr (~74 MBq) than what we have used in our previous studies (~185 MBq). This was found to be adequate in terms of image quality for clinically feasible emission times, ranging from 4-8 minutes per bed position. As radiation dose is directly proportional to administered activity, this represents a significant reduction in actual (mGy) dose compared to our previous studies. It is also of note that several investigators including equipment manufacturers are developing new advanced methods of image reconstruction that should result in further significant reductions in radiation dose. The radiation exposures generated by radiolabeled antibody PET tracers would be justified if they produce clinically valuable information.

Imaging of ^{89}Zr-pertuzumab was best performed 5-8 days following tracer administration. Scans on earlier days had higher liver and blood pool backgrounds and tended to have lower tumor uptake. The combination of higher tumor uptake and lower background on 5-8 day imaging has been observed with other antibody tracers (*15,16*). The multiple-day delay in blood pool clearance of antibody tracers can be considered a limitation of this technology. Potential alternatives include affibodies (*19*) and nanobodies (*20,21*), which have rapid biodistribution, allowing for imaging within hours of tracer administration. Affibodies and nanobodies labelled with shorter half-life tracers may have the added advantage of lower radiation dose to patients.

Although limited activity was seen in the bowel, we anticipate that this was the primary route for ^{89}Zr-pertuzumab excretion that did occur. Little measureable change was observed in

whole body activity following the first void (98% ± 1.8 of pre-void measurement) and there was no visualization of activity in the urinary bladder at any time.

One potential clinical application of ^{89}Zr-pertuzumab PET/CT is the assessment of HER2 status of disease, which may not be accessible by biopsy; for example, brain metastases. This becomes increasingly important given the recent finding that in patients with HER2-negative primary breast cancer who develop brain metastases, 20% will acquire HER2-positive metastases (*7*). Thus, a method of non-invasive, whole body screening for HER2-positive disease would be of clinical value as a predictive biomarker (*22*), helping to select patients for HER2-targeted therapy based on imaging. In this small trial, patients 1 and 5 had both HER2-positive and HER2-negative primary breast cancers and brain metastases. ^{89}Zr-pertuzumab PET/CT imaging suggested that the brain metastases were HER2-positive, one with histologic proof.

Another potential clinical application of ^{89}Zr-pertuzumab PET/CT is the assessment of HER2 heterogeneity. Patient 4 had a biopsy-proven HER2-negative primary breast malignancy, but a biopsy-proven HER2-positive chest wall metastases. Two previous liver biopsies in this patient were HER2-negative. The only site of ^{89}Zr-pertuzumab avidity was the chest wall lesion, which was the only site of known HER2-postive disease as defined by American Society of Clinical Oncology criteria. Of course, not all sites of malignancy had histologic analysis, but this early work suggests that ^{89}Zr-pertuzumab could assess heterogeneous HER2 tumor burden.

This first-in-human pilot of ^{89}Zr-pertuzumab PET/CT has a sample size of only six patients and was primarily designed to provide normal tissue biodistribution and dosimetry data. Further information on the biodistribution of ^{89}Zr-pertuzumab in normal and malignant tissues will be generated in additional HER2-targeted imaging trials with this novel agent. Patients included in this trial had metastases that were often treated with systemic therapy, often

including HER2-targeted therapy, prior to trial enrollment. This introduces difficulties in comparing extent of active malignancy with radiotracer uptake. A treated HER2-positive metastasis may not have sufficient residual active tumor to visualize on PET. Despite this limitation, five of six patients demonstrated sites of disease that were avid for ^{89}Zr-pertuzumab. Patients who had previously received, and were currently receiving, HER2-targeted therapy still demonstrated ^{89}Zr-pertuzumab-avid lesions. The effects of HER2-targeted therapy on ^{89}Zr-pertuzumab are not known; however, it was clear that HER2-targeted therapy did not prevent HER2-targeted imaging with ^{89}Zr-pertuzumab.

CONCLUSION

This first-in-human trial demonstrates that ^{89}Zr-pertuzumab PET/CT may be safely performed and has the potential to be a clinically valuable HER2-targeted imaging agent for patients with metastatic breast cancer. Potential clinical applications include assessment of HER2 status of lesions which may not be accessible to biopsy and assessment of HER2 heterogeneity. ^{89}Zr-pertuzumab PET/CT will next be utilized in a prospective clinical trial of patients with HER2-negative primary breast cancer, in order to analyze the ability of ^{89}Zr-pertuzumab to detect unsuspected HER2-positive metastatic disease and help direct HER2 targeted therapy to appropriate patients.

ACKNOWLEDGMENTS

We acknowledge funding from the Department of Defense Breast Cancer Research Program Breakthrough Award BC132676 (GAU), NIH R01 CA204167 (GAU, JSL) and a Genentech research grant (GAU). The authors gratefully acknowledge the Memorial Sloan Kettering Cancer Center Radiochemistry and Molecular Imaging Probe Core (NIH grant P30 CA08748) for additional support.

REFERENCES

1. Slamon DJ, Clark GM, Wong SG, Levin WJ, Ullrich A, McGuire WL. Human breast cancer: correlation of relapse and survival with amplification of the HER-2/neu oncogene. *Science (New York, NY).* 1987;235:177-182.

2. Slamon DJ, Leyland-Jones B, Shak S, et al. Use of chemotherapy plus a monoclonal antibody against HER2 for metastatic breast cancer that overexpresses HER2. *N Engl J Med.* 2001;344:783-792.

3. Romond EH, Perez EA, Bryant J, et al. Trastuzumab plus adjuvant chemotherapy for operable HER2-positive breast cancer. *N Engl J Med.* 2005;353:1673-1684.

4. Henry KE, Ulaner GA, Lewis JS. Human epidermal growth factor receptor 2-targeted PET/SPECT imaging of breast cancer: noninvasive measurement of a biomarker integral to tumor treatment and prognosis. *PET Clin.* 2017;12:269-288.

5. Ulaner GA, Hyman DM, Ross DS, et al. Detection of HER2-positive metastases in patients with HER2-negative primary breast cancer using 89Zr-trastuzumab PET/CT. *J Nucl Med.* 2016;57:1523-1528.

6. Ulaner GA, Hyman DM, Lyashchenko SK, Lewis JS, JA C. 89Zr-trastuzumab PET/CT for detection of HER2-positive metastases in patients with HER2-negative primary breast cancer. *Clin Nucl Med. epub ahead of print.*

7. Priedigkeit N, Hartmaier RJ, Chen Y, et al. Intrinsic subtype switching and acquired ERBB2/HER2 amplifications and mutations in breast cancer brain metastases. *JAMA Oncol.* 2017;3:666-671.

8. Hudis CA. Trastuzumab--mechanism of action and use in clinical practice. *N Engl J Med.* 2007;357:39-51.

9. Marquez BV, Ikotun OF, Zheleznyak A, et al. Evaluation of (89)Zr-pertuzumab in breast cancer xenografts. *Mol Pharm.* 2014;11:3988-3995.

10. Wolff AC, Hammond ME, Hicks DG, et al. Recommendations for human epidermal growth factor receptor 2 testing in breast cancer: American Society of Clinical Oncology/College of American Pathologists clinical practice guideline update. *J Clin Oncol.* 2013;31:3997-4013.

11. Vosjan MJ, Perk LR, Visser GW, et al. Conjugation and radiolabeling of monoclonal antibodies with zirconium-89 for PET imaging using the bifunctional chelate p-isothiocyanatobenzyl-desferrioxamine. *Nat Protoc.* 2010;5:739-743.

12. Holland JP, Sheh Y, Lewis JS. Standardized methods for the production of high specific-activity zirconium-89. *Nucl Med and Bio.* 2009;36:729-739.

13. Deri MA, Zeglis BM, Francesconi LC, Lewis JS. PET imaging with (89)Zr: from radiochemistry to the clinic. *Nucl Med and Bio.* 2013;40:3-14.

14. Barrett PH, Bell BM, Cobelli C, et al. SAAM II: Simulation, analysis, and modeling software for tracer and pharmacokinetic studies. *Metabolism.* 1998;47:484-492.

15. Pandit-Taskar N, O'Donoghue JA, Beylergil V, et al. (89)Zr-huJ591 immuno-PET imaging in patients with advanced metastatic prostate cancer. *Eur J Nucl Med Mol Imaging.* 2014;41:2093-2105.

16. O'Donoghue JA, Lewis JS, Pandit-Taskar N, et al. Pharmacokinetics, biodistribution, and radiation dosimetry for 89Zr-trastuzumab in patients with esophagogastric cancer. *J Nucl Med.* 2017. *Epub ahead of print.*

17. Sgouros G, Stabin M, Erdi Y, et al. Red marrow dosimetry for radiolabeled antibodies that bind to marrow, bone, or blood components. *Med Phys.* 2000;27:2150-2164.

18. Stabin MG, Sparks RB, Crowe E. OLINDA/EXM: the second-generation personal computer software for internal dose assessment in nuclear medicine. *J Nucl Med.* 2005;46:1023-1027.

19. Sorensen J, Sandberg D, Sandstrom M, et al. First-in-human molecular imaging of HER2 expression in breast cancer metastases using the 111In-ABY-025 affibody molecule. *J Nucl Med.* 2014;55:730-735.

20. Keyaerts M, Xavier C, Heemskerk J, et al. Phase I Study of 68Ga-HER2-nanobody for PET/CT assessment of HER2 expression in breast carcinoma. *J Nucl Med.* 2016;57:27-33.

21. Xavier C, Vaneycken I, D'Huyvetter M, et al. Synthesis, preclinical validation, dosimetry, and toxicity of 68Ga-NOTA-anti-HER2 nanobodies for iPET imaging of HER2 receptor expression in cancer. *J Nucl Med.* 2013;54:776-784.

22. Ulaner GA, Riedl CC, Dickler MN, Jhaveri K, Pandit-Taskar N, Weber W. Molecular imaging of biomarkers in breast cancer. *J Nucl Med.* 2016;57 Suppl 1:53S-59S.

FIGURE LEGENDS

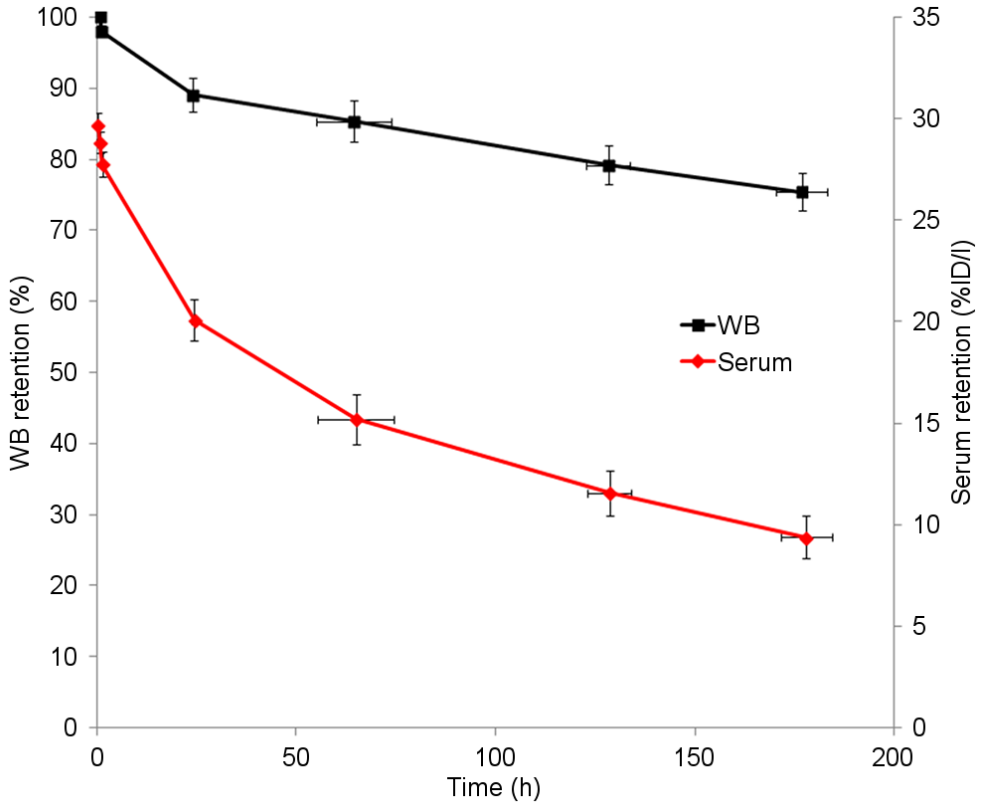

Figure 1. Summed whole body and serum biologic clearance data for ^{89}Zr-pertuzumab in six patients. Error bars indicate standard error of mean.

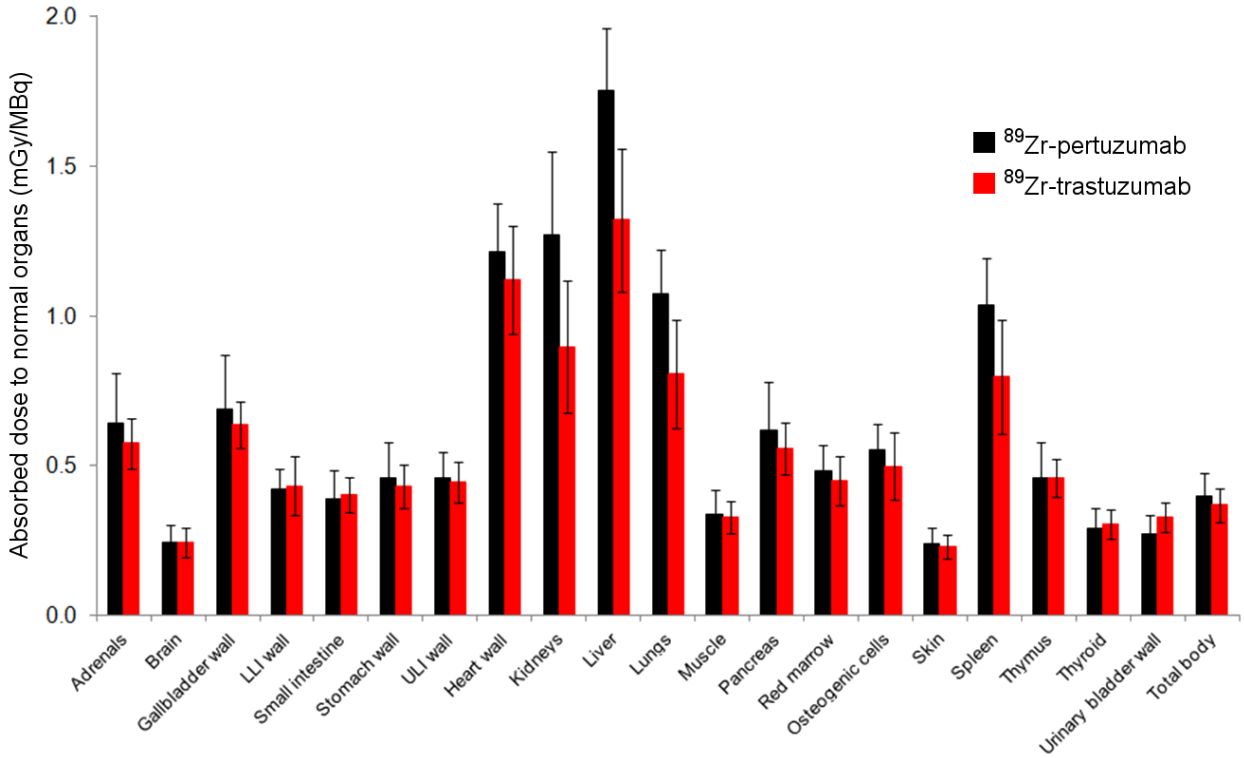

Figure 2. Comparative distributions of absorbed dose for ^{89}Zr-pertuzumab and ^{89}Zr-trastuzumab (*16*). Error bars denote standard deviations.

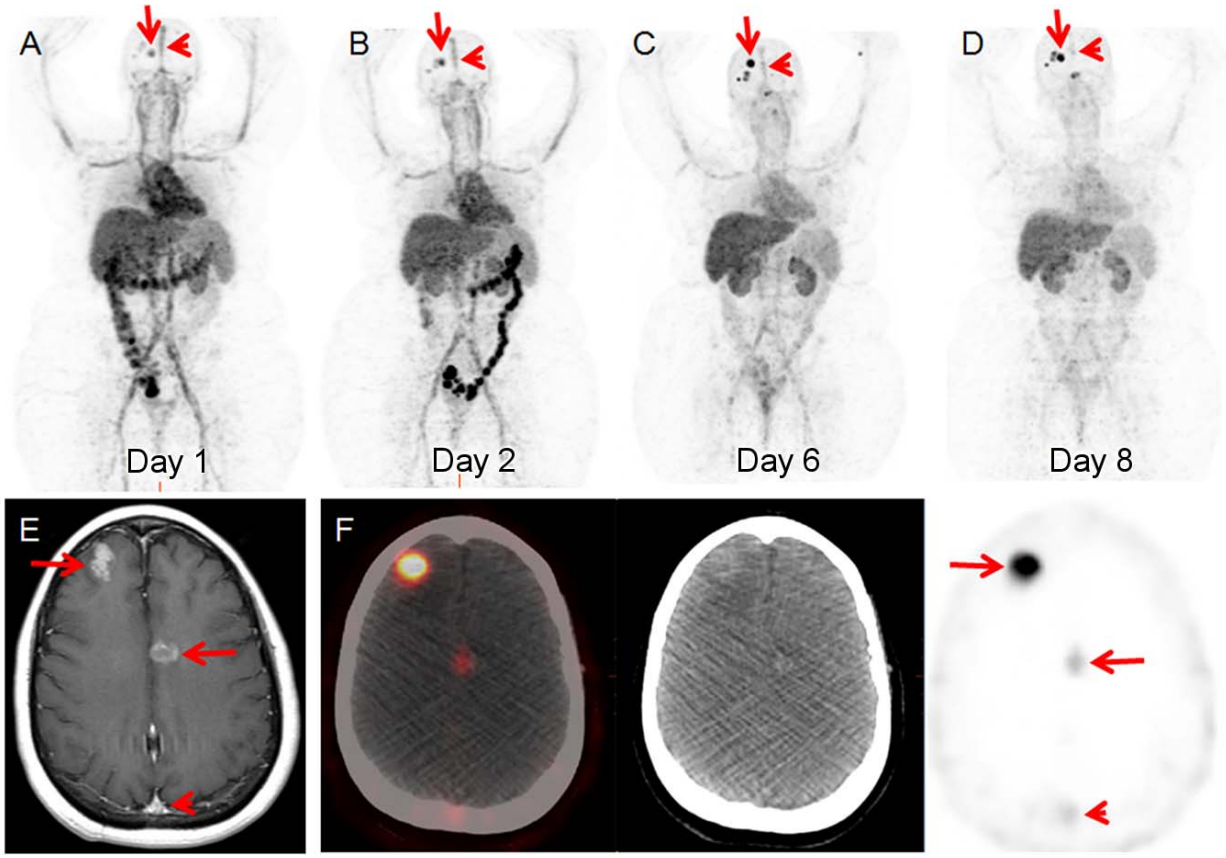

Figure 3. 46-year-old woman with both HER2-positive and HER2-negative primary breast malignancies and recently diagnosed brain metastases. Sequential maximum-intensity projection (MIP) images (A) 1 day, (B) 2 days, (C) 6 days, and (D) 8 days following administration of ^{89}Zr-pertuzumab. Blood pool and liver background clears on sequential images. Excreted bowel activity is seen on days 1 and 2. Bilateral kidney activity is visualized on all days. Increasing activity in foci overlying the skull is seen as time progresses (arrows). Decreasing activity is seen in the blood pool of the superior sagittal sinus (arrowheads). (E) Gadolinium-enhanced T1 weighed MR of the brain demonstrates enhancing brain metastases (arrows) and the superior sagittal sinus (arrowhead). (F) Axial fused PET/CT, CT, and PET images 8 days following ^{89}Zr-pertuzumab administration demonstrate avidity in the brain metastases (arrows) and minimal residual avidity in the superior sagittal sinus (arrowhead).

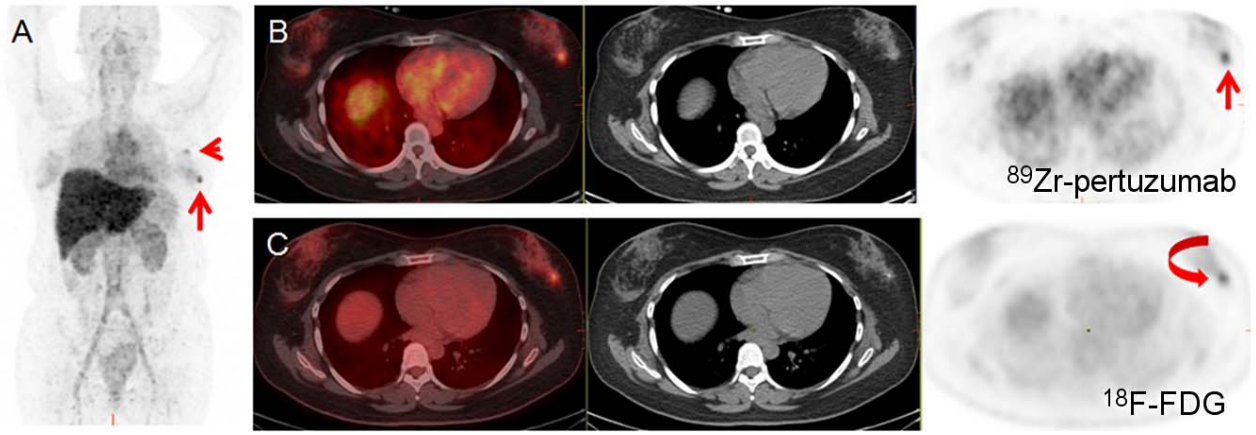

Figure 4. 58-year-old woman with HER2-positive breast cancer and current left breast and left axillary nodal disease. (A) MIP image 6 days following administration of ^{89}Zr-pertuzumab demonstrates the ^{89}Zr-pertuzumab-avid left breast (arrow) and left axillary nodal (arrowhead) disease. (B) Axial fused PET/CT, CT, and PET images obtained six days following ^{89}Zr-pertuzumab administration localize the ^{89}Zr-pertuzumab avidity in the left breast. (C) Axial fused PET/CT, CT, and PET images from a 18F-FDG PET/CT scan three weeks prior demonstrates the corresponding 18F-FDG-avid breast lesion.

Table 1: Characteristics of the Six Women with Invasive Ductal Breast Cancer

Patient	Age	Gender	Known Sites of Malignancy at Time of ^{89}Zr-pertuzumab Administration	Days Post-^{89}Zr-pertuzumab Administration of PET/CT Imaging	Sites of Demonstrably ^{89}Zr-pertuzumab-avid Disease
1	46	Female	Brain	1, 2, 6, 8	Brain
2	68	Female	Nodal	1, 2, 5, 7	Nodal
3	58	Female	Breast, nodal	1, 2, 6, 7	Breast, nodal
4	69	Female	Liver, bone, chest wall	1, 4, 5, 8	Chest wall
5	38	Female	Brain, lung, nodal, liver	1, 2, 5	Brain, lung, nodal
6	42	Female	Nodal	1, 4, 5, 7	None

Table 2: Summary Statistics for Whole Body and Serum Clearance

	Whole Body		Serum					
	$T_{1/2}$ eff	$T_{1/2}$ bio	A1 (%/L)	$T_{1/2}$ α eff	$T_{1/2}$ α bio	A2 (%/L)	$T_{1/2}$ β eff	$T_{1/2}$ β bio
Mean	67.7	521	12.6	12.1	15.5	17.3	59.3	201
SD	2.3	145	5.3	7.8	11.5	5.0	10.3	72
Median	66.9	456	13.0	9.7	11.2	16.3	55.5	176
Min	65.2	387	5.6	3.1	3.3	11.7	50.4	141
Max	70.8	730	18.8	22.1	30.8	23.3	78.4	322

Notes: Whole body clearance was mono-exponential. Serum clearance was bi-exponential conforming to the equation A1exp(- a1t)+A2exp(- a2t). A1 and A2 are partition coefficients and the respective $T_{½}$ values correspond to ln(2)/a. All half-times are in units of h.

Table 3: Absorbed Dose Estimates (mGy/MBq) for Normal Tissues

Target Organ	Mean	SD	Median	Min	Max
Adrenals	0.64	0.17	0.69	0.31	0.80
Brain	0.25	0.06	0.24	0.15	0.33
Breasts	0.33	0.08	0.35	0.18	0.41
Gallbladder Wall	0.69	0.18	0.72	0.34	0.83
Lower Large Intestinal Wall	0.42	0.06	0.40	0.36	0.52
Small Intestine	0.39	0.09	0.40	0.22	0.51
Stomach Wall	0.46	0.12	0.49	0.23	0.59
Upper Large Intestinal Wall	0.46	0.09	0.47	0.30	0.57
Heart Wall	1.22	0.16	1.24	0.98	1.37
Kidneys	1.27	0.28	1.18	0.98	1.64
Liver	1.75	0.21	1.73	1.54	2.13
Lungs	1.07	0.15	1.07	0.84	1.25
Muscle	0.34	0.08	0.35	0.19	0.44
Ovaries	0.38	0.10	0.38	0.20	0.50
Pancreas	0.62	0.16	0.66	0.30	0.77
Red Marrow	0.48	0.09	0.50	0.34	0.60
Osteogenic Cells	0.55	0.09	0.54	0.44	0.71
Skin	0.24	0.05	0.24	0.14	0.31
Spleen	1.04	0.16	1.01	0.87	1.26
Thymus	0.46	0.12	0.48	0.23	0.58
Thyroid	0.29	0.07	0.29	0.17	0.38
Urinary Bladder Wall	0.27	0.06	0.27	0.17	0.36
Uterus	0.37	0.10	0.37	0.19	0.49
Total Body	0.40	0.08	0.41	0.25	0.49
Effective Dose Equivalent (mSv/MBq)	0.72	0.09	0.73	0.56	0.83
Effective Dose (mSv/MBq)	0.54	0.07	0.56	0.41	0.62